

# Experimental and numerical assessment of biological soil improvement on the bearing capacity of shallow foundations

Javad Bidgoli<sup>1</sup>, Ahad Bagherzadeh Khalkhali<sup>\*1</sup>, Ali Derakhshani<sup>2</sup> and Amin Bahmanpour<sup>1</sup>

<sup>1</sup>Department of Civil Engineering, SR.C., Islamic Azad University, Tehran, Iran

<sup>2</sup>Department of Civil Engineering, Shahed University, Tehran, Iran

(Received December 1, 2024, Revised November 25, 2025, Accepted November 27, 2025)

**Abstract.** Shallow foundations are widely used where surface soils can sustain structural loads without excessive settlement. Various ground improvement methods, such as microbially induced carbonate precipitation (MICP), can increase bearing capacity in cases where soil strength is insufficient. MICP promotes the formation of calcium carbonate between soil particles, thereby improving interparticle bonding and enhancing soil strength. This study uses experimental testing and numerical analysis to examine the impact of a biologically treated thin layer on the ultimate bearing capacity and failure mechanisms of rectangular shallow foundations in sandy soils. Laboratory tests were conducted in a steel container measuring 100 cm in length, 70 cm in height, and 70 cm in width, examining the effects of different bacterial strains and varying treatment depths. Results show that bacterial inoculation and subsequent MICP treatment significantly increase the cohesion and strength of sandy soils. Introducing a biologically improved layer can increase the bearing capacity by up to three times. Positioning the treated layer at the surface yields a bearing capacity more than 10% higher than placing it at half the effective depth. Among the tested bacteria, *Bacillus megaterium* notably improves the soil's shear strength parameters compared to *Sporosarcina pasteurii*, resulting in an over 50% increase in foundation-bearing capacity. Numerical simulations using PLAXIS, based on the mohr-coulomb constitutive model, closely match the experimental findings, with a deviation of less than 10%.

**Keywords:** bearing capacity; MICP; PLAXIS; sandy soil; shallow foundation

## 1. Introduction

Bio-mediated soil improvement relies on biochemical processes that generate calcite precipitates within the soil matrix, thereby improving specific engineering properties (DeJong *et al.* 2010, Faruqi *et al.* 2023, Qabany *et al.* 2014, Mujah *et al.* 2017). Recent research confirms the method's effectiveness and environmental viability, supporting its potential for broader application in geotechnical engineering (DeJong *et al.* 2010, Umar *et al.* 2016). This technique offers promising mitigation for geohazards such as liquefaction and landslides in loose sandy soils, which frequently compromise foundation performance (Alvarado 2009). Biological treatments have proven successful in various geotechnical applications, including improvements in shear strength, reductions in permeability (Whiffin *et al.* 2007, Ivanov and Chu 2008, Harkes *et al.* 2010, van Paassen 2011), increased concrete strength and durability, remediation of structural cracks (Qian *et al.* 2010, Achal *et al.* 2013), and the cementation of sand columns to improve soil behavior (Cheng *et al.* 2023, Achal *et al.* 2009, Dhimi *et al.* 2013).

In recent years, interdisciplinary approaches integrating civil engineering, chemistry, and microbiology have been developed to modify subsurface soil properties (Whiffin *et*

*al.* 2007, Ivanov and Chu 2008, Mitchell and Santamarina 2005). One such technique, microbially induced calcite precipitation (MICP), promotes the formation of calcium carbonate within the soil matrix. The precipitated calcium carbonate binds soil particles, increasing strength and reducing hydraulic conductivity. MICP offers a practical solution for improving soil performance to support new and existing structures, with demonstrated applications in liquefiable sand deposits, slope stabilization, and subgrade reinforcement (DeJong *et al.* 2006, Cheng *et al.* 2013). While MICP has also been proposed for enhancing erosion resistance, relatively few experimental and numerical investigations have assessed its effectiveness in improving surface erosion resistance (Ham *et al.* 2023, Li *et al.* 2023).

Researchers have investigated bio-mediated soil improvement through small-scale laboratory experiments and theoretical studies. For example, Tsukamoto and Oda (2013) examined microbial calcium carbonate precipitation in Toyoura sand at relative densities of 30%, 60%, and 85%, reporting that lower densities resulted in greater calcium carbonate accumulation. This was attributed to improved bacterial absorption and nutrient distribution in looser soils containing more voids. Cheng *et al.* (2014) corroborated these results, observing that increased soil density enhances the uniaxial compressive strength of treated samples, as denser particle arrangements enable calcium carbonate crystals to form more continuous bridges between grains. Kim and Park (2017) assessed bio-mediated treatment in sandy soils at relative densities of 40%, 60%, and 80%, as well as in silty and gravelly soils at various compaction

\*Corresponding author, Ph.D.

E-mail: a-bagherzadeh@srbiau.ac.ir

levels. Their findings indicated that sandy soil exhibited the highest calcium carbonate precipitation at 60% density, while both lower and higher densities produced less due to suboptimal particle packing. In silt specimens, significant variation in precipitation was observed only at a 90% density.

Sharma and Ramakrishnan (2016) investigated the effects of MICP on the strength of fine-grained soils by evaluating variables such as *Bacillus pasteurii* concentration, the strength of the cementation solution, and treatment duration. Following immersion periods ranging from 3 to 7 days, unconfined compressive strength (UCS) tests showed that MICP improved the strength of CH-type soils more significantly than CL-type soils. Longer treatment durations and higher bacterial concentrations resulted in greater strength gains. Meng *et al.* (2021) applied the MICP technique to reduce wind-induced surface soil erosion in desert environments, emphasizing its stabilization performance. The underlying soil must provide sufficient strength and bearing capacity to support structural foundations, ensuring long-term stability.

Kulanthaivel *et al.* (2022) investigated the impact of *Sporosarcina pasteurii* and *Lysinibacillus fusiformis*, isolated from eggshells and combined with calcium chloride, on the strength characteristics of sand. Using varying molarities of the cementing agent (0.25, 0.50, 0.75, and 1.0 M), they observed that the unconfined compressive strength of the treated sand reached approximately 650 kPa. The optimal improvement in Young's modulus and calcium carbonate content was recorded at 28.9 MPa and 17.9%, respectively, when the sand was treated with *S. pasteurii* and a 0.50 M concentration of the eggshell-derived cementing solution.

Although MICP has shown considerable potential, certain soils, particularly in layered formations, exhibit low shear strength and require targeted improvement strategies. Askari *et al.* (2022) investigated the influence of thin, weak and strong layers on the bearing capacity of shallow foundations, concluding that weak layers reduce capacity, while strong layers contribute to its improvement. However, the effect of bio-mediated treatment in thin layers on foundation capacity has received limited attention in large-scale experimental and numerical studies. Furthermore, most existing research places the improved layer at a constant depth, with minimal investigation into how variations in its placement influence bearing capacity (Yu *et al.* 2021, Terzis and Laloui 2019).

Gowthaman *et al.* (2022) proposed a hybrid model known as *B-EICP* that combines bacterial and enzymatic processes for stabilizing fine-grained slope soils. Their results showed that enzyme-assisted MICP can accelerate calcite precipitation and improve cohesion in silty slopes. This research extended the traditional bacterial MICP framework into finer soils and slope applications. Nevertheless, the complexity of controlling enzyme activity and long-term durability remained unresolved.

Ezzat *et al.* (2023) performed a critical review summarizing more than 200 global MICP studies, categorizing them into lab-scale, pilot-scale, and field-scale applications. They concluded that MICP is still

underutilized in practical geotechnical projects due to injection challenges, heterogeneity in calcite formation, and insufficient studies on different soil textures. They also proposed the need for comparative experiments across soil types and bacterial cultures.

Ouyang *et al.* (2022) conducted a detailed investigation into the effects of microbial content on compaction, swelling, and strength characteristics of expansive soils using MICP treatment. Their results showed that increasing the bacterial concentration led to greater calcium carbonate deposition, resulting in reduced swelling potential and higher unconfined compressive strength. This study provided strong experimental evidence for the feasibility of MICP in problematic expansive soils. However, it focused mainly on *laboratory-scale testing* and a single soil type (expansive clay), with limited discussion on bacterial types or injection uniformity.

Zhang *et al.* (2023) presented a global review of MICP applications for soil stabilization, focusing on mechanisms, influencing factors, and large-scale feasibility. They emphasized that although MICP has been effective in strengthening sandy soils, challenges remain in controlling calcite precipitation patterns and ensuring uniform cementation across heterogeneous soil structures. The review also pointed out that variations in pH, nutrient concentration, and bacterial species significantly affect MICP efficiency.

Liu *et al.* (2024) investigated the role of MICP in improving the strength of low-cohesive soils. They performed both microscopic (SEM and XRD) and macroscopic analyses to identify the relationship between calcite morphology and mechanical enhancement. Their work confirmed that particle size distribution strongly governs bacterial movement and crystal growth. However, the authors highlighted the need for more data on fine-grained soils and different bacterial strains to generalize the results.

Zhu *et al.* (2024) reported that bacterial characteristics, including urease activity, cell concentration, and interaction with calcium carbonate, directly influence the efficiency of the MICP process. Bacteria with high urease activity decompose urea into ammonium and carbonate ions, thereby increasing the pH of the surrounding environment and promoting the precipitation of calcium carbonate. The precipitated calcium carbonate functions as a cementing agent, increasing soil cohesion and interparticle bonding and improving the soil's mechanical strength and load-bearing capacity.

This study aims to identify the optimal placement of a bio-mediated soil layer using laboratory experiments and numerical modeling. The methodology includes constructing a physical model of sandy soil with a thin bio-treated layer over which a rectangular foundation is positioned. The foundation's bearing capacity is systematically examined under varying conditions, including bacterial strains and treatment layer depths. Finally, the results from the physical model tests are compared with those obtained from numerical simulations, providing a comprehensive evaluation of the treatment's effectiveness.

## 2. Research methodology

### 2.1 Similarity theory and model design principles

In geotechnical physical modeling, the behavior of a scaled model should represent that of the prototype according to similarity theory. The fundamental similarity ratios adopted in this study are summarized as follows (Eqs. (1) to (5))

$$\text{Geometric similarity: } \lambda_L = L_m/L_p \quad (1)$$

$$\text{Density similarity: } \lambda_\rho = \rho_m/\rho_p \quad (2)$$

$$\text{Stress similarity: } \lambda_\sigma = \lambda_\rho \lambda_L g_m/g_p \quad (3)$$

$$\text{Elastic modulus similarity: } \lambda_E = \lambda_\sigma/\lambda_\epsilon \quad (4)$$

$$\text{Bearing capacity similarity: } \lambda_q = \lambda_\sigma \quad (5)$$

where subscripts *m* and *p* denote the model and the prototype, respectively, and  $g_m = g_p$  for a 1 g test. Under 1 g conditions, exact stress similarity cannot be achieved; nevertheless, by maintaining the same material type and density as in the prototype, and by adjusting geometric dimensions and applied load levels according to  $\lambda_L$ , the stress field distribution can approximate similitude behavior.

In this study, the geometric scale ratio between the model and the field prototype was  $\lambda_L = 1/15$ . Although the 1g model cannot fully satisfy complete similarity, these scaling relationships ensured that the observed load–settlement and failure patterns remain representative of the prototype foundation behavior.

### 2.2 Physical laboratory modeling

This section outlines the laboratory testing procedures, including testing apparatus, loading methods, soil characteristics, and bacterial properties. Physical modeling is employed to investigate the geotechnical behavior of soil under controlled conditions. The study utilizes specialized geotechnical equipment to construct physical models under standard gravitational acceleration (1 g), allowing for the systematic evaluation of soil improvement effects.

#### 2.2.1 Testing equipment

For physical modeling, a steel container with internal dimensions of 100 cm in length, 70 cm in height, and 70 cm in width was fabricated, as illustrated in Fig. 1(a). In this study, *D* denotes depth (bio-treated layer) as illustrated in Fig. 1(a). A precipitation box was installed at the top of the loading frame to achieve the target soil density, allowing sand to fall freely from a height of 60 cm. The physical model tests in this study were conducted using a steel strip footing to represent the behavior of a shallow foundation with negligible deformation. The footing was machined from a single piece of mild steel and had dimensions of 700 mm (length) × 70 mm (width) × 10 mm (thickness). The physical and mechanical properties of the footing material are listed in Table 1.

Table 1 Mechanical properties of the footing

Property	Symbol	Value	Unit
Elastic modulus	<i>E</i>	2e+8	Kpa
Poisson's ratio	<i>v</i>	0.15	–

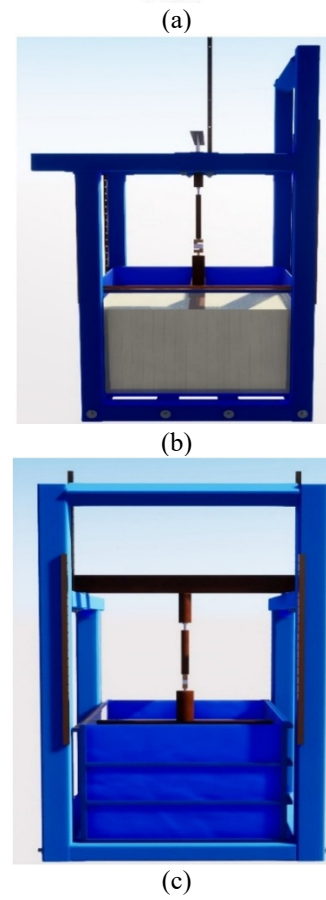
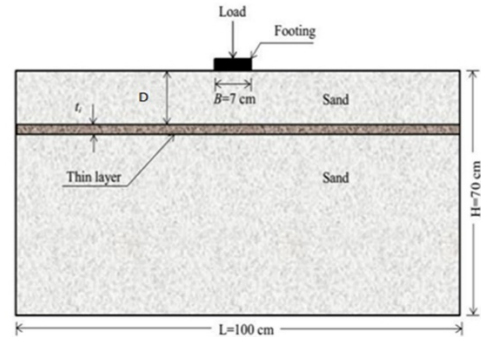


Fig. 1 (a) Schematic of the physical modeling apparatus used in this study for testing the rectangular foundation; (b) and (c) represent two different views of the loading system

The ratio of footing stiffness to that of the treated soil ( $E_f / E_s > 1000$ ) indicates that the footing behaves as a rigid foundation during loading. The self-weight of the steel footing was negligible compared to the total applied load increments, and its deformation under loading was insignificant. These parameters were also adopted in the numerical PLAXIS model to maintain consistency between the experimental and numerical analyses within the framework of similarity theory.

In the experiment, load was applied to the foundation using a manual hydraulic jack at a controlled rate of 1 mm/min. As shown in Fig. 1(b), a 50 kN load cell positioned on the jack piston recorded the applied load. A dial gauge with a precision of 0.01 mm was used to measure the foundation's settlement. Fig. 1(c) illustrates the complete physical model setup, featuring a rectangular foundation positioned on a sandy soil bed.

### 2.2.2 Scale conversion laws

Physical modeling in geotechnical engineering is typically classified into two categories: modeling under standard gravitational acceleration (1 g) and modeling under elevated acceleration levels (ng) using a geotechnical centrifuge. Muir Wood (2004) comprehensively summarized the scale relationships applicable to both 1 g and ng conditions. While strict adherence to established scaling laws improves model accuracy, achieving geometric and material similarity in model construction is equally critical. This study builds on the work of Askari *et al.* (2022), applying their validated scale factor of 1:15. This scaling approach accounts for essential parameters, including the thickness of the steel foundation plate, loading conditions, and spacing of the cross-sections.

### 2.2.3 Geotechnical characterization of the sand

The sand used in this study was sourced from silty sand deposits located in Hamadan Province and was tested in an air-dried condition. The particle size distribution is presented in Fig. 2(a). Based on the Unified Soil Classification System (USCS), the material is categorized as poorly graded sand (SP). The key physical properties of the sand are provided in Table 2. The relative density was determined according to ASTM D4253-00 (ASTM 2004a, b). Given the siliceous nature of the sand and the relatively low stress levels applied during physical modeling, significant particle crushing is not anticipated.

The shear strength parameters of the sand were determined through direct shear and triaxial tests, as illustrated in Fig. 2(b). The direct shear test results indicate negligible cohesion, measured at approximately 0.4 kPa. The internal friction angle of the sand is 48 degrees. In addition, the triaxial test yielded a cohesion value of 5 kPa and an internal friction angle of 36 degrees.

### 2.2.4 Bacteria and microorganisms used

*Sporosarcina pasteurii* (formerly *Bacillus pasteurii*) and *Bacillus megaterium* are Gram-positive, non-pathogenic bacteria capable of inducing calcite precipitation. These microorganisms produce high levels of urease, an enzyme that hydrolyzes urea into carbonate and ammonia. *Bacillus megaterium* strains will be sourced from the Iranian Collection Center of Fungi and Industrial Bacteria in this study. These bacteria have been widely used in previous soil improvement applications. The bacterial cell surface carries a negative charge due to the presence of hydroxide ions, enabling the adsorption of positively charged calcium ions. Upon the introduction of urea into the bacterial environment, hydrolysis produces carbonate ions, which subsequently react with calcium ions to form calcium carbonate.

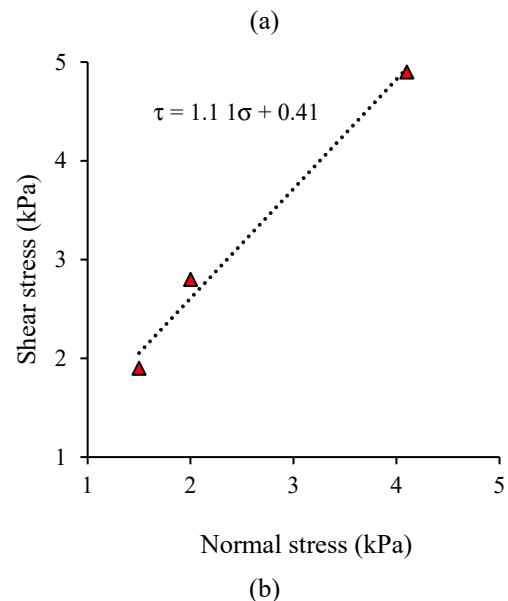
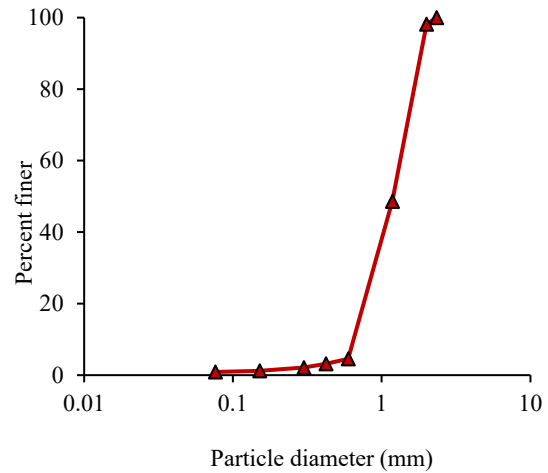


Fig. 2 (a) Grain size distribution curve and (b) direct shear test results for the sandy soil used in this study

Table 2 Physical properties of sand in experimental tests

Soil parameters	value
$D_{max}$ (mm)	2.38
$D_{60}$ (mm)	1.45
$D_{30}$ (mm)	0.90
$D_{10}$ (mm)	0.67
$C_u$	2.16
$C_c$	0.83
$G_s$	2.66
$D_r$ (%)	41.00
$\gamma_{d,max}$ (kN/m <sup>3</sup> )	19.85
$\gamma_{d,min}$ (kN/m <sup>3</sup> )	13.73
$\gamma_d$ (kN/m <sup>3</sup> )	15.71
Soil classification (USCS)	SP

Among *Bacillus* species, *Sporosarcina pasteurii* is the most widely recognized for its high urease activity and ability to hydrolyze urea. The efficiency of the MICP process depends on several key factors, including pH, temperature, urea concentration, and the availability of

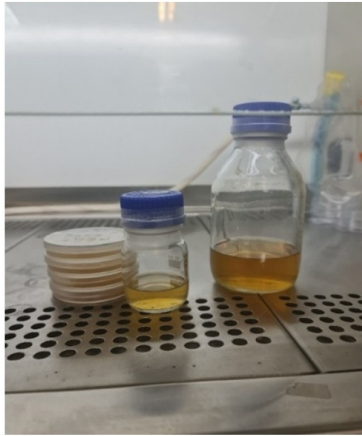


Fig. 3 *Bacillus megaterium* cultivation in the laboratory

calcium ions. Gram-positive bacteria are particularly well-suited for this application due to their thick, peptidoglycan-rich cell walls, which allow them to withstand osmotic stress. The most effective MICP treatment typically involves a cementation solution containing both urea and a calcium source, which promotes urease activity and increases the soil pH, thereby facilitating the precipitation of calcium carbonate.

This study employed the Gram-positive bacteria *Sporosarcina pasteurii* (ATCC 11859) and *Bacillus megaterium* (ATCC 14581), capable of surviving in alkaline, calcium-rich environments. The bacterial culture medium was prepared according to Tryptic Soy Broth (TSB) protocols, as the National Center for Biotechnology Information (NCBI) recommended.

### 2.2.5 Preparation, cultivation, and injection procedure of bacteria

Tryptic soy broth (TSB) was prepared and sterilized in an autoclave at 121°C for 15 min, then it was incubated at 30 °C and all subsequent handling was performed under a laminar flow hood. *Bacillus megaterium* (ATCC 14581) and *Sporosarcina pasteurii* (ATCC 11859) were cultivated at 30°C for 24 h. For *S. pasteurii*, the culture medium was supplemented with 20 g/L urea. The initial pH of the medium was adjusted to 7.5, and cultures were agitated at 150 rpm until reaching  $OD_{600} \approx 1.2-1.4$  ( $\approx 10^8$  cells/mL). An example of *Bacillus megaterium* cultivation in the laboratory is shown in Fig. 3.

The cementation solution consisted of 1.5 M  $CaCl_2$  and 3 M urea and was introduced in three treatment cycles. Bacterial suspension and cementation solution were applied in alternating fashion with 24 h intervals to promote uniform carbonate precipitation. Following the last application, specimens were cured for 28 days under controlled laboratory conditions (30°C; high relative humidity) prior to testing. Transport of the bacterial and cementation solutions through the sandy soil was governed primarily by gravity and capillary forces.

### 2.2.6 Physical modeling test program

Table 3 presents the key variables in the physical

Table 3 Various soil improvement scenarios using *Megaterium* and *Pasteurii* bacteria

Test ID	Type of bacteria	Zi (cm)
T1	No improvement	-
T2	<i>Megaterium</i>	0
T3	<i>Megaterium</i>	3.5
T4	<i>Pasteurii</i>	0
T5	<i>Pasteurii</i>	3.5

Table 4 Material properties of bacteria-treated sand used in numerical modeling after calibration by physical modeling

Soil material	Sand enriched with <i>Megaterium</i>	Sand enriched with <i>Pasteurii</i>
Cohesion (kPa)	72	41
Friction angle	45	40
Dry density ( $kN/m^3$ )	18.2	16.3
Elastic modulus ( $kN/m^2$ )	250	200
Poisson's ratio	0.35	0.3

modeling test program. The study includes five test series: the first utilizes untreated sand as a control, while the remaining four involve sand treated with bacterial solutions. The test parameters vary according to the bacterial strain and the bio-treated layer's placement depth.

### 2.3 Numerical modeling in PLAXIS

PLAXIS is a specialized geotechnical finite element software used for modeling and analyzing soil–structure interactions. It enables engineers to simulate the behavior of soil and rock under various loading and construction conditions with high accuracy. This study analyses foundation behaviour using PLAXIS under plane strain conditions, applying the mohr-coulomb constitutive model.

The mohr-coulomb model is one of the most classical and widely used models in geotechnical analysis, implemented in PLAXIS 2D to simulate the mechanical behavior of soils. This model is based on the assumption of elastic–perfectly plastic behavior, meaning that soil behaves linearly and elastically up to the yield point, and beyond this limit, it enters the plastic and irreversible deformation zone. The elastic behavior in this model is defined by two parameters: the Young's modulus ( $E$ ) and Poisson's ratio ( $\nu$ ), which represent the stiffness and the recoverable deformation capacity of the soil. The plastic behavior, on the other hand, is governed by the mohr-coulomb failure criterion, which relates soil failure to its two main strength parameters - the internal friction angle ( $\phi$ ) and cohesion ( $c$ ).

As outlined in Table 3, the numerical model comprises five configurations: one untreated scenario, two surface-treated cases using different bacterial strains, and two configurations where bio-mediated layers are placed at a depth of  $Z_i$ . These cases are examined individually in the subsequent section. Since the bio-treated layers have distinct mechanical properties, their input parameters are defined separately. The properties used for modeling the bio-mediated soil layers are presented in Table 4.

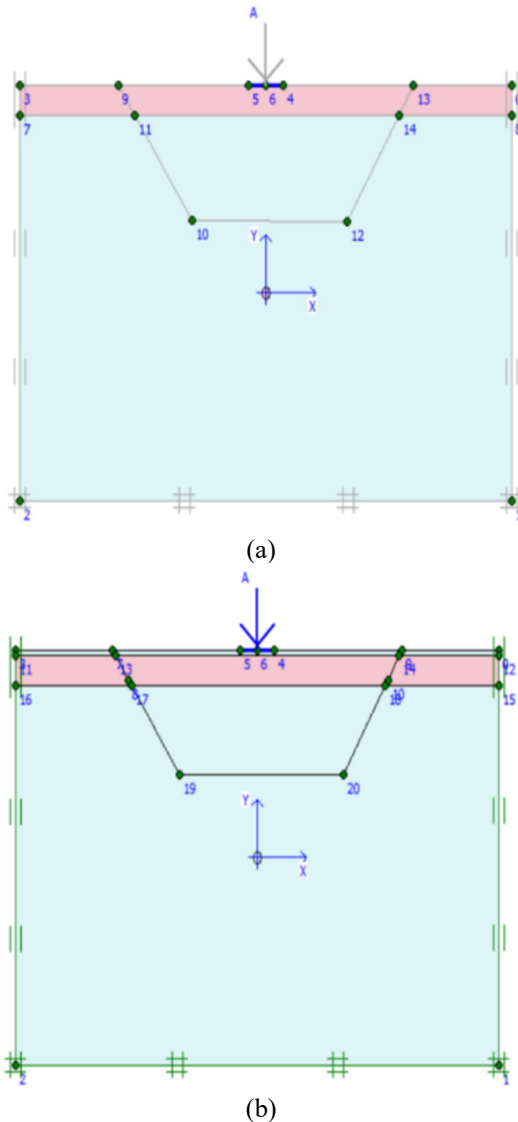


Fig. 4 Numerical model of a rectangular foundation with a bio-treated layer located at (a) the soil surface and (b) an effective depth of 3.5 cm below the foundation

The foundation length is 7 cm, consistent with the physical model. A static load is applied to simulate failure conditions and to compute the ultimate bearing capacity using PLAXIS.

The shear strength parameters of the bio-treated sands, including cohesion and internal friction angle, were determined using direct shear tests conducted after a 28-day curing period. The dry unit weights of the treated layers were measured in accordance with ASTM D4253-00, using the relative density and compaction methods. The elastic modulus values for the bacteria-treated sand were estimated from the stress–strain response observed during the physical plate load tests and further refined through calibration of the numerical model to closely match the experimental pressure–settlement behavior. Poisson’s ratios were selected based on literature values reported for biologically treated sandy soils (e.g., DeJong *et al.* 2010, Kim and Park 2017) and adjusted slightly to reflect observed deformation characteristics in the PLAXIS simulations.

For material modeling in PLAXIS, 15-node triangular elements were used to construct the mesh. Mesh density was varied across different zones to balance computational efficiency with modeling accuracy. A finer mesh was applied in regions near the foundation and within the thin improved layers to increase precision, while a coarser mesh was used in the surrounding areas to reduce computation time. Figs. 4(a) and 4(b) present the finite element configurations before loading. Fig. 4(a) shows the model with the improved layer positioned directly beneath the foundation, whereas Fig. 4(b) depicts the configuration with the bio-treated layer located at a depth of 3.5 cm.

In the following, the sensitivity analysis for both the treated and untreated soil samples with *Bacillus megaterium* is presented. This analysis was conducted to investigate the influence of key mohr–coulomb model parameters on the numerical simulation results.

In the untreated sample, variations in the elastic modulus ( $E$ ) exhibit an almost perfectly linear behavior across the  $\pm 25\%$  range, with a negligible effect on bearing capacity. Increasing  $E$  by 25% results in only a 0.64% rise in  $q_u$  (from 395 to 397.52 kPa), while a 25% reduction decreases  $q_u$  by about 0.84% (to 391.67 kPa). In contrast, cohesion ( $c$ ) shows a more noticeable influence. The bearing capacity changes almost linearly within  $\pm 15\%$ , but from +20% to +25%, the trend becomes slightly nonlinear with a steeper slope. A 25% increase in  $c$  raises  $q_u$  by about 9.1% (to 430.96 kPa), while a 25% decrease lowers it by around 9.4% (to 357.92 kPa). The internal friction angle ( $\phi$ ) demonstrates the strongest and most nonlinear effect. Increasing  $\phi$  from  $36^\circ$  to  $45^\circ$  (+25%) significantly increases  $q_u$  by approximately 30.7% (to 516.10 kPa), whereas reducing  $\phi$  to  $27^\circ$  (–25%) decreases  $q_u$  by about 16.3% (to 330.47 kPa). Therefore, in the untreated soil,  $\phi$  is the most sensitive and nonlinear parameter governing the bearing capacity,  $c$  has a moderate and mostly linear effect, and  $E$  has the least influence on  $q_u$ , affecting mainly the deformation rather than the strength.

In the treated sample, the behavior of the parameters in relation to bearing capacity becomes significantly more stable and consistent compared to the untreated condition. The variation of elastic modulus ( $E$ ) within  $\pm 25\%$  shows an almost perfectly linear trend with a very small influence on  $q_u$ . When  $E$  increases by 25% (from 250 to 312.5 kN/m<sup>2</sup>), the bearing capacity rises from 1250 kPa to 1261.87 kPa, equivalent to a +0.94% increase, while a 25% reduction in  $E$  decreases  $q_u$  to 1238.22 kPa (–0.95%). Cohesion ( $c$ ) also exhibits a nearly linear relationship with  $q_u$ ; a 25% increase in  $c$  (from 72 to 90 kPa) raises the bearing capacity to 1256.95 kPa (+0.56%), and a 25% decrease (to 54 kPa) lowers it to 1240.86 kPa (–0.73%). The internal friction angle ( $\phi$ ) remains the most influential parameter but shows a more linear and stable behavior compared with the untreated sample. Increasing  $\phi$  from  $45^\circ$  to  $56.25^\circ$  (+25%) results in a rise of  $q_u$  to 1272.31 kPa (+1.77%), while decreasing  $\phi$  to  $33.75^\circ$  (–25%) reduces  $q_u$  to 1232.54 kPa (–1.40%). Overall, in the MICP-treated soil with *Bacillus megaterium*, the sensitivity of the bearing capacity to variations in  $\phi$ ,  $c$ , and  $E$  has clearly decreased, and the overall response of the mohr–coulomb parameters is more stable, nearly linear, and less prone to uncertainty.

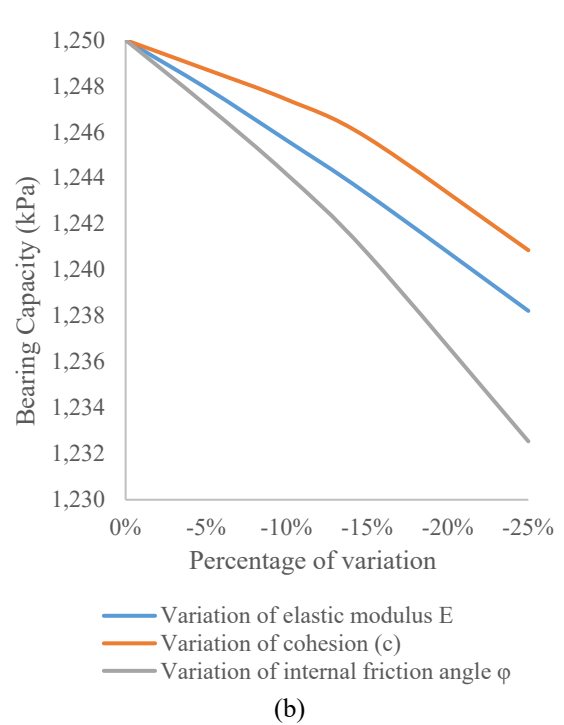
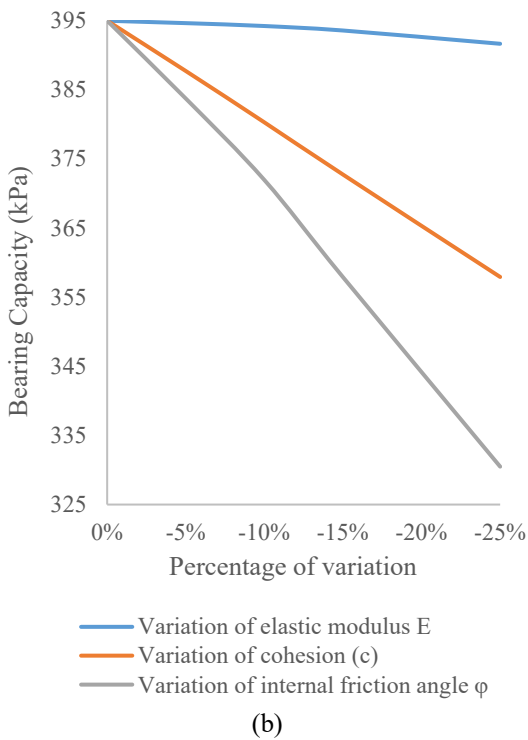
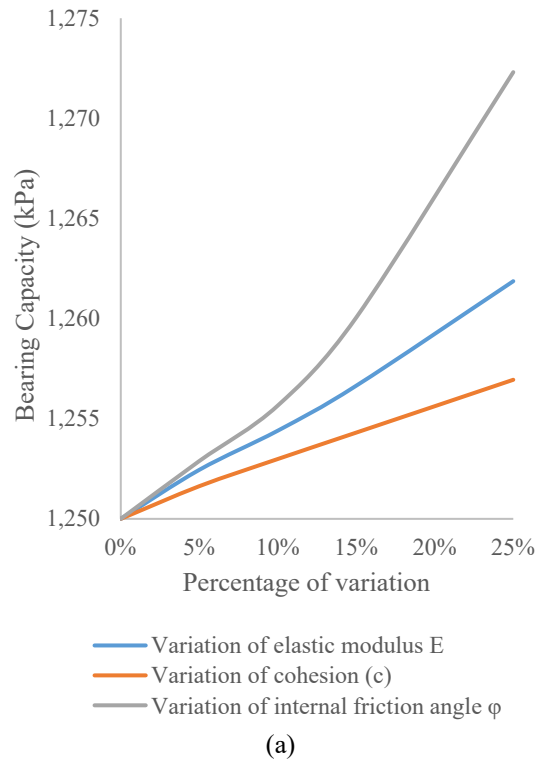
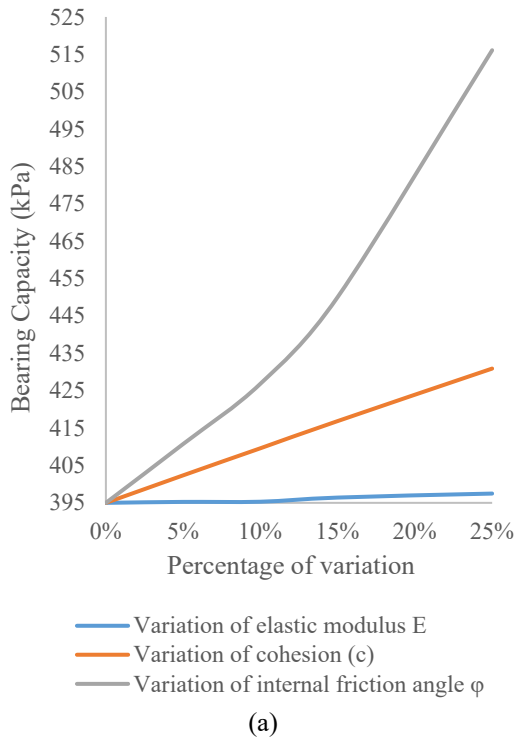


Fig. 5 Sensitivity analysis values for the untreated sample (a) Variation 0 to +25% and (b) Variation 0 to -25%

Fig. 6 Sensitivity analysis values for the treated sample (a) Variation 0 to +25% and (b) Variation 0 to -25%

Figs. 5 and 6 shows Sensitivity analysis values for the untreated and treated sample.

### 3. Results and discussion

#### 3.1 Foundation behavior on untreated sandy soil

Laboratory evaluations were conducted after soil preparation and bacterial cultivation within the loading apparatus. In this setup, a 1 kPa load applied to the model corresponds to a real-world stress of 4.88 kPa. Therefore, the actual bearing capacity is determined by multiplying the measured test results by a factor of 4.88.

A loading test on a foundation placed over untreated silica sand recorded a failure load of approximately

Table 5 Calculated values in Meyerhof's equations

Bearing Capacity Factors		Shape Factors	
$N_q$	222.30	$K_p$	6.79
$N_c$	199.26	$s_c$	1.1
$N_\gamma$	526.45	$s_q = s_\gamma$	1.05

460 kPa, resulting in a calculated bearing capacity of 95 kPa for the rectangular foundation. Using Meyerhof's equations, as outlined in Eqs. (6) to (8), the ultimate bearing capacity of the foundation is calculated to be 390 kPa. When the maximum dry unit weight ( $\gamma_{dmax} = 19.85 \text{ kN/m}^3$ ) is used instead of the average unit weight ( $\gamma = 15.7 \text{ kN/m}^3$ ), the bearing capacity increases to 470 kPa. The Hansen and Vesic correction factors were set to 1.0, assuming a strip foundation under general conditions, which results in consistent bearing capacity values across all three analytical models. The experimental bearing capacity (460 kPa) falls within the theoretical range (390–470 kPa). This variation can be attributed to differences in unit weight, soil condition, degree of compaction, and the inherent assumptions in theoretical models versus actual field behavior. Overall, the experimental findings align well with Meyerhof's and other empirical formulations, indicating no significant discrepancy.

As shown in Fig. 7(a), the rupture wedge forms uniformly beneath the foundation, with the recorded settlement reaching approximately 8.7 mm. Fig. 7(b) presents the pressure–settlement curve corresponding to the rectangular foundation. The following section compares these experimental results with those obtained from numerical modeling.

$$\begin{aligned} N_q &= e^{\pi \tan \phi} \tan^2(45 + \phi/2) \rightarrow N_c \\ &= (N_q - 1) \cot \phi, N_\gamma \\ &= (N_q - 1) \tan(1.4\phi) \end{aligned} \quad (6)$$

$$\begin{aligned} K_p &= \tan^2(45 + \phi/2) \rightarrow s_c \\ &= 1 + (0.2)(K_p)(B/L), s_q \\ &= s_\gamma = 1 + (0.1)(K_p)(B/L) \end{aligned} \quad (7)$$

$$\begin{aligned} q_{ult} &= c N_c s_c d_c + q N_q s_q d_q \\ &\quad + 0.5 \gamma' B N_\gamma s_\gamma d_\gamma \end{aligned} \quad (8)$$

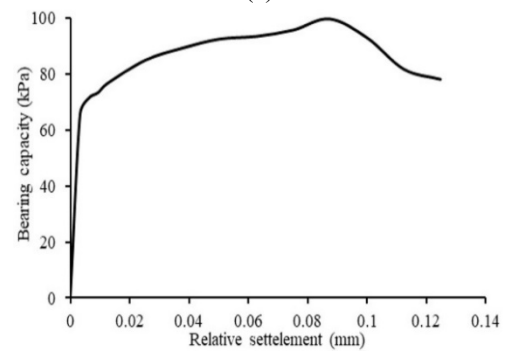
In Meyerhof's equations  $N_q$ ,  $N_c$  and  $N_\gamma$  represent the bearing capacity factors while  $s_c$ ,  $s_q$  and  $s_\gamma$  denote the shape factors. The depth factors in these equations are assumed to be 1. The calculated values in the analysis are presented in Table 5.

### 3.2 Foundation behavior on sandy soil with a *bacillus megaterium*-enriched layer

This experiment placed a thin bio-treated layer enriched with *Bacillus megaterium* directly beneath the foundation. Based on the findings of Askari *et al.* (2022), the primary



(a)



(b)

Fig. 7 (a) Failure zone formation and (b) bearing capacity–settlement curve for a rectangular foundation on untreated sandy soils

influence of an improved thin layer is expected under these conditions. The layer was stabilized by injecting a cementation solution containing *B. megaterium*, prepared by dissolving 180 g of calcium chloride and 180 g of urea in one liter of water.

Following soil treatment and a curing period of 28 days, loading tests were performed to assess bearing capacity and settlement. The measured resistance was 1380 kPa, representing a 200% increase relative to the untreated condition. The failure occurred at a settlement of 8.8 mm. The failure zone exhibited noticeable fragmentation and brittleness in the surrounding soil, as illustrated in Fig. 8(a).

In the subsequent test, the *bacillus megaterium*-enhanced thin layer was positioned at half the effective foundation depth, 3.5 cm below the surface. The treated sample was subjected to loading following soil preparation and a 28-day curing period. The measured bearing capacity was 1170 kPa (equivalent to 243 kPa in real), representing an approximate 154% increase compared to the untreated T1 sample. Failure occurred at a settlement of 8.7 mm, as shown in Fig. 8(b). The corresponding bearing capacity and relative settlement curve for the foundation resting on *B. megaterium*-treated sand are presented in Fig. 8(c).

### 3.3 Foundation behavior on sandy soil with a *sporosarcina pasteurii*-enriched layer

In this test series, *Sporosarcina pasteurii* was used to

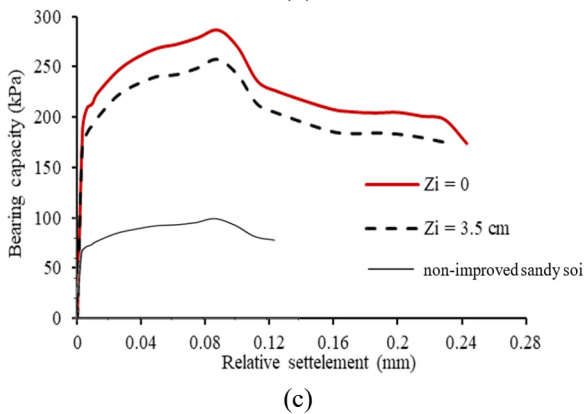
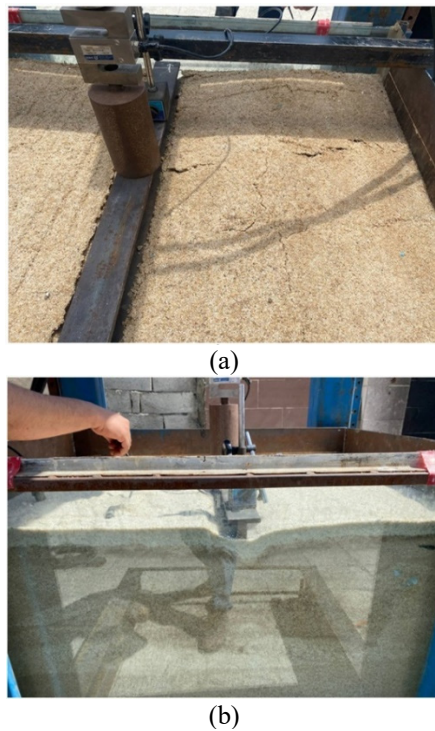


Fig. 8 (a) Failure pattern in sandy soil treated with *Bacillus megaterium* beneath the foundation surface, (b) failure zone when the treated layer is placed at half the effective depth and (c) bearing capacity–settlement curve for foundations on *B. megaterium*-improved sand

improve the mechanical properties of sandy soil. After a 28-day curing period, the treated soil exhibited a cohesion value of 4 kPa, notably lower than the 5 kPa observed in soil treated with *Bacillus megaterium*. The internal friction angles were measured at 43° for *B. megaterium*-treated soil and 41° for *S. pasteurii*-treated soil.

When the bio-treated layer was applied at the surface, directly beneath the foundation, the bearing capacity increased to 900 kPa (equivalent to 187 kPa), representing a 96% improvement over the untreated condition. However, this increase was substantially lower than that achieved with *B. megaterium*. The failure occurred at a settlement of 8.7 mm, and the failure zone exhibited brittle characteristics, as shown in Fig. 9(a).

In contrast, when the *Sporosarcina pasteurii*-treated layer was positioned at a depth of 3.5 cm, the ultimate

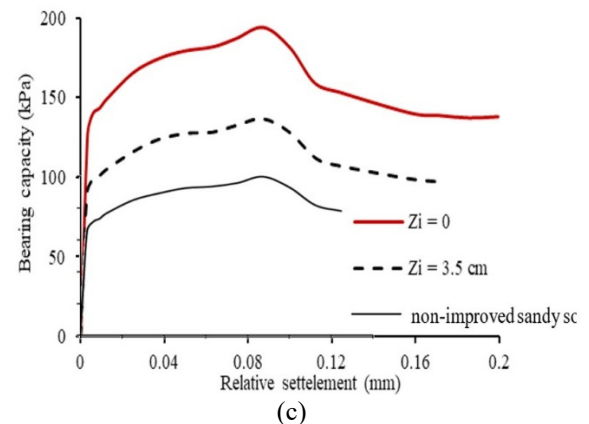


Fig. 9 Failure zone and bearing behavior of a rectangular foundation on *Sporosarcina pasteurii*-treated sandy soil: (a) treated layer at the surface, (b) treated layer at a depth of 3.5 cm, and (c) bearing capacity–settlement curve

bearing capacity of the rectangular foundation reached 813 kPa (equivalent to 169 kPa), reflecting a 77% increase compared to the untreated condition. The failure occurred at a settlement of 8.7 mm, with the failure mode shown in Fig. 9(b). Fig. 9(c) presents the corresponding bearing capacity–settlement curve for the foundation on *S. pasteurii*-treated soil. Overall, the results demonstrate that *Bacillus megaterium* contributes more significantly to improving foundation-bearing capacity than *Sporosarcina pasteurii* under the conditions tested.

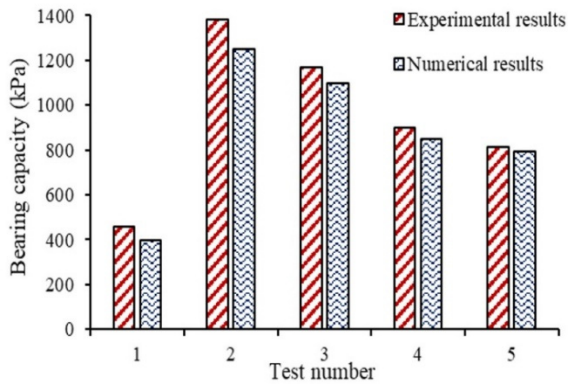


Fig. 10 Comparison of numerical and experimental results

### 3.4 Comparison of numerical and experimental results

In the untreated condition, the physical model yielded a bearing capacity of 460 kPa, while the numerical model estimated a capacity of 395 kPa. Fig. 10 compares numerical simulation results and experimental findings across all test configurations.

For *Bacillus megaterium*-treated soil:

- With the improved layer positioned at the surface, the physical model recorded a bearing pressure of 1380 kPa, while the numerical model estimated 1250 kPa.
- When the treated layer was placed at a depth of 3.5 cm, the physical and numerical models recorded bearing pressures of 1170 kPa and 1100 kPa, respectively.

For *Sporosarcina pasteurii*-treated soil:

- When the bio-treated layer was at the surface, the physical model recorded a bearing pressure of 900 kPa, while the numerical model estimated 850 kPa.
- At a depth of 3.5 cm, the corresponding values were 813 kPa for the physical model and 795 kPa for the numerical model.

### 3.5 Discussion and key findings

As shown in Fig. 11, The percentage of variation between the three experiments was 3-6%. This was limited to 3-5% for the other tests, and the final results are presented in Figs. 7 to 9, based on the minimum values, with a standard deviation of approximately 6.76 for the three values. If the fluctuation in the data (3 to 5%) and the accuracy of the measuring instruments are considered as criteria, the maximum error value is equivalent to 6.64 kPa, which corresponds to 7% of the final recorded value for the unreinforced bearing capacity, and 3.5% of the final recorded value for the reinforced condition.

Failure mechanisms and stress-strain behavior: The failure behavior of both untreated and MICP-treated sandy soils exhibited distinct characteristics. Fig. 12 presents the stress-strain curves derived from the Physical test data. In untreated sand, the load-settlement relationship showed a gradual increase in stress followed by ductile failure, indicating continuous plastic deformation and redistribution of stresses.

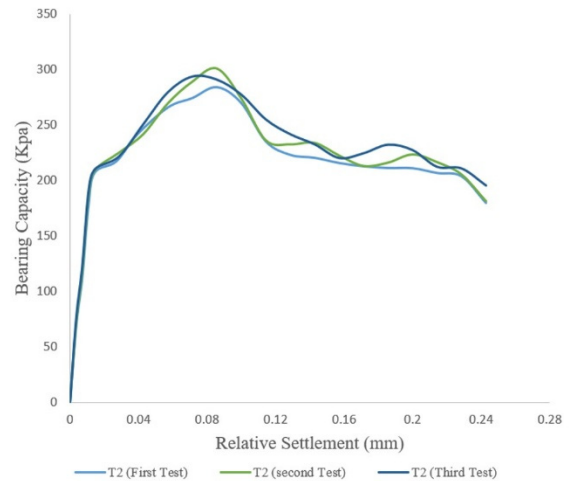


Fig. 11 Stress-strain curve for T2 Test experiments (treated with megatrium at the surface)

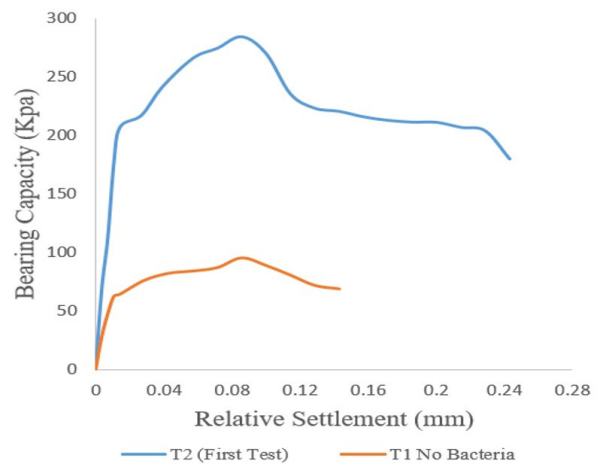


Fig. 12 Stress-Strain Curve for Treated and Untreated Conditions

In contrast, MICP-treated samples exhibited steeper initial slopes and sharper post-peak reductions, reflecting an increase in stiffness and a transition toward brittle failure. The enhanced interparticle bonding due to calcium carbonate precipitation limited particle rearrangement, resulting in higher bearing capacity but reduced ductility.

The observed failure patterns also confirm this transition. When the bio-treated layer was positioned at the surface, failure primarily occurred through a localized punching and brittle mechanism directly beneath the foundation. However, when the treated layer was placed at mid-depth (3.5 cm), the failure surface expanded laterally, resembling a general shear mode. An example of fracture types in T1 and T2 tests is presented in Fig. 13.

The experimental and numerical results clearly demonstrate the significant influence of microbial soil improvement on the bearing behavior of shallow foundations. Among the tested bacteria, *Bacillus megaterium* provided superior enhancement, with more than a 50% increase in bearing capacity compared to *Sporosarcina pasteurii*. This is attributed to the higher calcium carbonate precipitation achieved by *B. megaterium*,

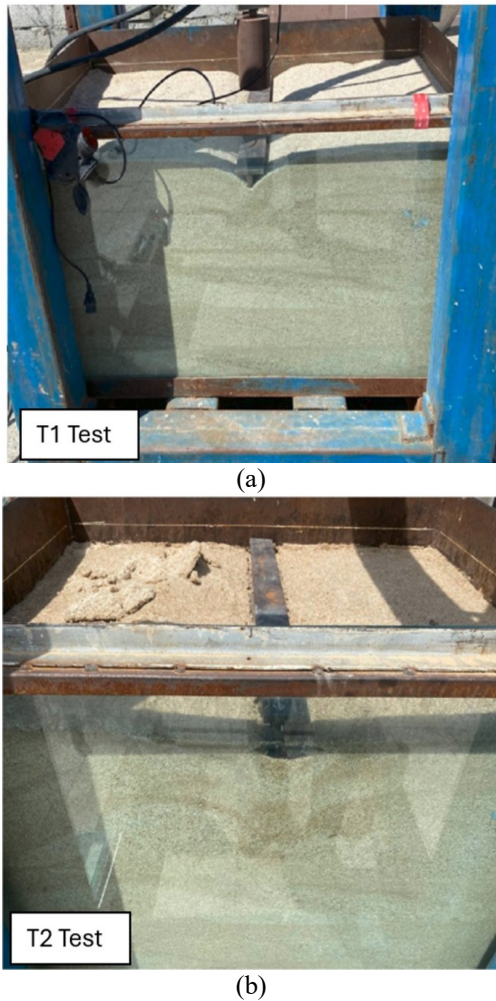


Fig. 13 Failure in (a) test T1 and (b) test T2

which improved both cohesion and friction angle more effectively.

The bearing capacity improvement is mainly governed by increases in cohesion ( $c'$ ) and internal friction angle ( $\phi'$ ), both of which directly impact the bearing capacity factors ( $N_c$ ,  $N_q$ ,  $N_\gamma$ ) in classical theories such as Meyerhof and Hansen. Specifically, the enhanced cohesion contributed significantly to the observed capacity gains in treated samples.

Additionally, the positioning of the bio-treated layer has a direct effect on the failure mechanism. When the treated layer was placed at the surface, the failure pattern resembled punching shear, characterized by localized vertical deformation beneath the footing. In contrast, placing the treated layer at a depth of 3.5 cm resulted in a general shear failure, with a wider failure zone and more gradual load redistribution. These observations highlight the importance of layer placement for achieving optimal performance.

The agreement between experimental and numerical results (within 10%) also confirms the validity of the mechanical parameters used in modeling and the reliability of the mohr-coulomb model in simulating bio-improved soil behavior under shallow foundation loading.

Based on these findings, the sand with the above-mentioned properties was used in the physical model, where it led to a 200% increase in bearing capacity, corresponding to 190 kPa, for the strip footing. Since a full (prototype) scale was not available for direct evaluation, the bearing capacity calculations for a large-scale footing (presented below) also confirm an increase of 243%, equal to 2268 kPa. This is in good agreement with the bearing capacity calculations for the small-scale footing using Meyerhof's method. The calculations are as follows.

Bearing capacity of the untreated specimen by Meyerhof's method:

$$q_u = C \cdot N_c \cdot Sc \cdot dc + q \cdot N_q \cdot sq \cdot dq + 0.5 \cdot \gamma \cdot B' \cdot N_\gamma \cdot sy \cdot dy$$

$$N_c = (N_q - 1) \cot \phi = 50.59$$

$$N_q = e^{\pi \tan \phi} \tan^2 \left( 45 + \frac{\phi}{2} \right) = 37.75$$

$$N_\gamma = (N_q - 1) \tan(1.4\phi) = 44.43$$

$$\text{Considering } C = 5 \text{ and } q = \gamma \cdot D_f = 0,$$

$$(q_u)_{model} = 5 * 50.59 * 1.08 + 0.5 * 15.71 * 0.07 * 44.43 * 1.05 = 291.2 \text{ kPa}$$

$$(q_u)_{prototype} = 5 * 50.59 * 1.08 + (0.5 * 15.71 * 0.07 * 44.43 * 1.05) * 15 = 658 \text{ kPa}$$

Bearing capacity of the sample treated with *megaterium*,  $c = 5 \text{ Kpa}$ ,  $\phi = 43^\circ$ .

$$(q'_u)_{model} = C \cdot N_c \cdot Sc \cdot dc + 0.5 \cdot \gamma \cdot B' \cdot N_\gamma \cdot sy \cdot dy$$

$$N_c = 105.11, N_q = 99.01, N_\gamma = 171.14$$

$$(q'_u)_{model} = 5 * 105.11 * 1.08 + 0.5 * 18.2 * 0.07 * 171.14 * 1.04 = 680.9 \text{ kPa}$$

$$(q'_u)_{prototype} = 5 * 105.11 * 1.08 + (0.5 * 18.2 * 0.07 * 171.14 * 1.04) * 15 = 2268.2 \text{ kPa}$$

Where:

- $(q_u)_{model}$  : Bearing capacity of small-scale modeling without enhancement
- $(q'_u)_{model}$  : Bearing capacity of small-scale modeling with biological enhancement
- $(q_u)_{prototype}$  : Bearing capacity of large-scale modeling without enhancement
- $(q'_u)_{prototype}$  : Bearing capacity of large-scale modeling with biological enhancement

Rokhman *et al.* in 2025 for infrastructure development often faces challenges due to soils with low bearing capacity, which can potentially cause instability and subsidence and threaten the safety of structures. Therefore, an efficient and environmentally friendly stabilization method is required. This study aims to evaluate the effectiveness of Microbial Induced Calcite Precipitation (MICP) in improving bearing capacity and soil strength through the formation of bacterial soil columns. This study employed a full-scale physical model test using 40 cm diameter and 200 cm deep soil columns filled with soil mixed with *Bacillus subtilis*, compacted, and cured for 56 days. The results showed significant improvements in the geotechnical characteristics of the soil, with CBR values increasing from 5.5% to over 12%, unconfined compressive strength reaching 345 kPa, and modulus of elasticity

increasing to 12.5 MPa. Soil cohesion increased to 65 kPa, while internal friction angle increased from 10° to 34°. The novelty of this research is the application of MICP technology in the form of bacterial soil columns as an innovative, effective, and sustainable stabilization method to improve the mechanical properties of soft soils. In addition, it means that increasing 260% of the bearing capacity. This is in the good agreement with the conclusion of our research (244%).

Finally, this study confirms that microbial soil improvement, especially with *B. megaterium*, can be an effective and sustainable method to enhance the bearing capacity of sandy soils, especially when applied strategically at the ground surface.

#### Key Findings:

- Numerical modeling demonstrated strong agreement with experimental results, indicating high predictive accuracy.
- *Bacillus megaterium*-treated layers improved bearing capacity more than *Sporosarcina pasteurii*-treated layers.
- Surface-level bio-treatment consistently resulted in higher bearing capacity than deeper or more extensive treatments.

## 4. Conclusions

This study investigated the effect of bio-mediated soil improvement on shallow foundations' bearing capacity using experimental and numerical approaches. Two bacterial strains, *Sporosarcina pasteurii* and *Bacillus megaterium*, were used to induce calcium carbonate precipitation within a thin sandy layer. The findings can be summarized as follows:

- The integration of a microbially improved thin layer beneath a shallow foundation can lead to up to a threefold increase in bearing capacity compared to untreated conditions. For *Bacillus megaterium*, the ultimate bearing capacity increased by 200% when the treated layer was located at the surface and by 154% when positioned at mid-depth ( $D = B / 2 = 3.5$  cm). For *Sporosarcina pasteurii*, the bearing capacity increased by 96% for surface treatment and 77% for mid-depth treatment. Thus, the surface-treated models exhibited bearing capacities about 18% (for *B. megaterium*) and 10.7% (for *S. pasteurii*) higher than those of the mid-depth cases.
- The placement depth of the bio-treated layer has a significant effect. When applied at the surface, bearing capacity improved by over 10% compared to the same layer embedded at half the foundation width.
- *Bacillus megaterium* outperformed *Sporosarcina pasteurii*, increasing cohesion and friction angle more significantly and enhancing load-bearing capacity by over 50%.
- The failure mode transitioned from punching shear to general shear as the depth of the improved layer increased, indicating a shift in soil behavior due to improved interparticle bonding.

- Numerical simulations using PLAXIS and the Mohr-Coulomb model showed excellent agreement (less than 10% deviation) with experimental results, confirming the validity of the chosen parameters and modeling approach.

Overall, the results demonstrate that bio-mediated treatment, particularly with *Bacillus megaterium*, offers a promising, sustainable, and effective solution for improving the mechanical performance of sandy soils under shallow foundations.

## References

- Achal, V., Mukerjee, A. and Reddy, M.S. (2013), "Biogenic treatment improves the durability and remediates the cracks in concrete structures", *Constr. Build. Mater.*, **48**, 1-5. <https://doi.org/10.1016/j.conbuildmat.2013.06.061>.
- Achal, V., Mukherjee, A., Basu, P.C. and Reddy, M.S. (2009), "Lactose mother liquor as an alternative nutrient source for microbial concrete production by *Sporosarcina pasteurii*", *J. Ind. Microbiol. Biot.*, **36**(3), 433-438. <https://doi.org/10.1007/s10295-008-0514-7>.
- Alvarado, D. (2009), "Bio-mediated soil improvement: Cementation of unsaturated sand samples", University of California: Davis, LA, USA.
- An, R., Gao, H., Zhang, X., Chen, X., Wang, Y. and Xu, H. (2024), "Mechanical behaviour and microstructure of granite residual bio-cemented soil by microbially induced calcite precipitation with different cementation solution concentrations", *Environ. Earth Sci.*, **83**(1), 31. <https://doi.org/10.1007/s12665-023-11352-w>.
- Askari, M., Bagherzadeh Khalkhali, A., Makarchian, M. and Ganjian, N. (2022), "Evaluation of the thin layer effect on the ultimate bearing capacity of strip foundations on sand amirkabir", *J. Civil Eng.*, **54**(7), 2681-2698. <https://doi.org/10.22060/ceej.2022.20657.7490>.
- Cheng, L., Cord-Ruwisch, R. and Shahin, M.A. (2013), "Cementation of sand soil by microbially induced calcite precipitation at various degrees of saturation", *Can. Geotech. J.*, **50**(1), 81-90. <https://doi.org/10.22060/ceej.2022.20657.7490>.
- Cheng, L., Shahin, M.A. and Cord-Ruwisch, R. (2014), "Bio-cementation of sandy soil using microbially induced carbonate precipitation for marine environments", *Géotechnique*, **64**(12), 1010-1013. <https://doi.org/10.1680/geot.14.T.025>.
- Cheng, Z. and Geng, X. (2023), "Mechanical behaviours of biopolymers reinforced natural soil", *Struct. Eng. Mech.*, **88**(2), 179-188. <https://doi.org/10.12989/sem.2023.88.2.179>.
- DeJong, J.T., Fritzsche, M.B. and Nüsslein, K. (2006), "Microbially induced cementation to control sand response to undrained shear", *J. Geotech. Geoenviron. Eng.*, **132**(11), 1381-1392. [https://doi.org/10.1061/\(ASCE\)1090-0241\(2006\)132:11\(1381\)](https://doi.org/10.1061/(ASCE)1090-0241(2006)132:11(1381)).
- DeJong, J.T., Mortensen, B.M., Martinez, B.C. and Nelson, D.C. (2010), "Bio-mediated soil improvement", *Ecol. Eng.*, **36**(2), 197-210. <https://doi.org/10.1016/j.ecoleng.2008.12.029>.
- Dhami, N.K., Reddy, M.S. and Mukherjee, A. (2013), "Biomineralization of calcium carbonates and their engineered applications: a review", *Frontiers in microbiology*, **4**, 314. <https://doi.org/10.3389/fmicb.2013.00314>.
- Ezzat, S.M. and Al-Ani, R. (2023), "A critical review on microbially induced carbonate precipitation for soil stabilization: The global experiences and future prospective", *Pedosphere*, **33**(4), 897-917. <https://doi.org/10.1016/j.pedsph.2022.12.006>.
- Faruqi, A., Hall, C.A. and Kendall, A. (2023), "Sustainability of bio-mediated and bio-inspired ground improvement techniques for geologic hazard mitigation: a systematic literature review", *Front. Earth Sci.*, **11**, 1211574. <https://doi.org/10.3389/feart.2023.1211574>.

- Gowthaman, S., Iki, T., Ichinohe, A., Nakashima, K. and Kawasaki, S. (2022), "Feasibility of bacterial-enzyme induced carbonate precipitation technology for stabilizing fine-grained slope soils", *Front. Built Environ.*, **8**, 1044598. <https://doi.org/10.3389/fbuil.2022.1044598>.
- Ham, S.M., Jeon, M.K. and Kwon, T.H. (2023), "Surface erosion of MICP-treated sands: Erosion function apparatus tests and CFD-DEM bonding model", *Geomech. Eng.*, **33**(2), 133-140. <https://doi.org/10.12989/gae.2023.33.2.133>.
- Harianto, T., Muhiddin, A.B. and Arsyad, A. (2025), "Bearing capacity and strength of bacterial soil columns full-scale tests", *Civil Eng. J.*, **11**(4), 1353-1370. <https://doi.org/10.28991/cej-2025-011-04-06>.
- Harkes, M.P., Van Paassen, L.A., Booster, J.L., Whiffin, V.S. and van Loosdrecht, M.C. (2010), "Fixation and distribution of bacterial activity in sand to induce carbonate precipitation for ground reinforcement", *Ecol. Eng.*, **36**(2), 112-117. <https://doi.org/10.1016/j.ecoleng.2009.01.004>.
- Ivanov, V. and Chu, J. (2008), "Applications of microorganisms to geotechnical engineering for bioclogging and biocementation of soil in situ", *Rev. Environ. Sci. Bio/Technol.*, **7**, 139-153. <https://doi.org/10.1007/s11157-007-9126-3>.
- Kim, D. and Park, K. (2017), "Evaluation of the grouting in the sandy ground using bio injection material", *Geomech. Eng.*, **12**(5), 739-752.
- Kulanthaivel, P., Soundara, B., Selvakumar, S. and Das, A. (2022), "Application of waste eggshell as a source of calcium in bacterial bio-cementation to enhance the engineering characteristics of sand", *Environ. Sci. Pollut. R.*, **29**(44), 66450-66461.
- Li, S., Huang, M., Cui, M., Lin, P., Xu, L. and Xu, K. (2023), "Stabilization of cement-soil utilizing microbially induced carbonate precipitation", *Geomech. Eng.*, **35**(1), 95. <https://doi.org/10.12989/gae.2023.35.1.095>.
- Liu, Z., Beng, J., Wu, Y., Nie, K., Dang, Y., Yao, Y., Li, J. and Fang, M. (2024), "Microbial induced calcite precipitation for improving low-cohesive soil: Mechanisms, methods and macroscopic properties", *Low-Carbon Mater. Green Constr.*, **2**(1). <https://doi.org/10.1007/s44242-024-00060-8>.
- Meng, H., Gao, Y., He, J., Qi, Y. and Hang, L. (2021), "Microbially induced carbonate precipitation for wind erosion control of desert soil: Field-scale tests", *Geoderma*, **383**, 114723. <https://doi.org/10.1016/j.geoderma.2020.114723>.
- Mitchell, J.K. and Santamarina, J.C. (2005), "Biological considerations in geotechnical engineering", *J. Geotech. Geoenviron. Eng.*, **131**(10), 1222-1233. [https://doi.org/10.1061/\(ASCE\)1090-0241\(2005\)131:10\(1222\)](https://doi.org/10.1061/(ASCE)1090-0241(2005)131:10(1222)).
- Mujah, D., Shahin, M.A. and Cheng, L. (2017), "State-of-the-art review of biocementation by microbially induced calcite precipitation (MICP) for soil stabilization", *Geomicrobiol. J.*, **34**(6), 524-537. <https://doi.org/10.1080/01490451.2016.1225866>.
- Qabany, A.A. and Soga, K. (2014), "Effect of chemical treatment used in MICP on engineering properties of cemented soils. In Bio-and chemo-mechanical processes in geotechnical engineering", *Géotechnique Symposium*, 107-115, ICE Publishing. <https://doi.org/10.1680/bcmpe.60531.010>.
- Ouyang, Q., Zhao, Y., Zhang, J. and Zhang, Y. (2022), "Experimental study on the influence of microbial content on compaction, swelling and strength characteristics of improved expansive soil", *Front. Earth Sci.*, **10**, 863357. <https://doi.org/10.3389/feart.2022.863357>.
- Qian, C., Wang, R., Cheng, L. and Wang, J. (2010), "Theory of microbial carbonate precipitation and its application in restoration of cement-based materials defects", *Chinese J. Chem.*, **28**(5), 847-857. <https://doi.org/10.1002/cjoc.201090156>.
- Rajasekar, A., Moy, C.K., Wilkinson, S. and Sekar, R. (2021), "Microbially induced calcite precipitation performance of multiple landfill indigenous bacteria compared to commercially available bacteria in porous media", *Plos one*, **16**(7), e0254676. <https://doi.org/10.1371/journal.pone.0254676>.
- Sharma, A. and Ramkrishnan, R. (2016), "Study on effect of microbial induced calcite precipitates on strength of fine grained soils", *Perspect. Sci.*, **8**, 198-202. <https://doi.org/10.1016/j.pisc.2016.03.017>.
- Terzis, D. and Laloui, L. (2019), "A decade of progress and turning points in the understanding of bio-improved soils: A review", *Geomech. Energ. Environ.*, **19**, 100116. <https://doi.org/10.1016/j.gete.2019.03.001>.
- Tsukamoto, M. and Oda, K. (2013), "Influence of relative density on microbial carbonate precipitation and mechanical properties of sand", *Proceedings of the 18th International Conference on Soil Mechanics and Geotechnical Engineering*, 2613-2616.
- Umar, M., Kassim, K.A. and Chiet, K.T.P. (2016), "Biological process of soil improvement in civil engineering: A review", *J. Rock Mech. Geotech. Eng.*, **8**(5), 767-774. <https://doi.org/10.1016/j.jrmge.2016.02.004>.
- Van Paassen, L.A. (2009), Biogrout, ground improvement by microbial induced carbonate precipitation.
- Whiffin, V. S., Van Paassen, L.A. and Harkes, M.P. (2007), "Microbial carbonate precipitation as a soil improvement technique", *Geomicrobiol. J.*, **24**(5), 417-423. <https://doi.org/10.1080/01490450701436505>.
- Wu, Q. and Wang, Y. (2025), "Influence of on-site low-ureolysis bacteria and high-ureolysis bacteria on the effectiveness of MICP processes", *J. Geotech. Geoenviron. Eng.*, **151**(1), 04024144. <https://doi.org/10.1061/JGGEFK.GTENG-12338>.
- Yu, T., Souli, H., Pechaud, Y. and Fleureau, J.M. (2021), "Review on engineering properties of MICP-treated soils", *Geomech. Eng.*, **27**(1), 13-30. <https://doi.org/10.12989/gae.2021.27.1.013>.
- Zhang, K., Liu, J. and Han, Y. (2023), "Microbial-Induced Carbonate Precipitation (MICP) technology: A review", *Environ. Sci. Pollut. R.*, **30**, 25465-25483. <https://doi.org/10.1007/s11356-023-24529-9>.
- Zhu, J., Wei, R., Peng, J. and Dai, D. (2024), "Improvement schemes for bacteria in MICP: A review", *Materials*, **17**(22), 5420. <https://doi.org/10.3390/ma17225420>.

IC